Spectrograph point spread function characterization using a sine comb generator: testing on the Keck Planet Finder spectrograph

David J. Erskine[a], Jerry Edelstein[b], Andrew W. Howard[c], Sam Halverson[d], Martin M. Sirk[b], and Ed H. Wishnow[b]

[a]Spectral Fringe, Oakland, CA, USA
[b]Space Sciences Lab, University of California, Berkeley, CA 94720, USA
[c]California Institute of Technology, 1200 E. California Blvd., Pasadena, CA 91125, USA
[d]NASA Jet Propulsion Laboratory, Pasadena, CA 91011, USA

ABSTRACT

We describe a technique for spectrograph characterization. An inexpensive Michelson interferometer, fiber connected and illuminated by white light, creates sine combs that illuminate every pixel along a spectrograph bandwidth. The sine comb visibility compared to its zero or low frequency value measures the modulation transfer function (MTF) of a spectrograph. This in turn yields the point spread function (PSF) width or spectral resolution. This method can sense the PSF in between lines of spectral lamps, for spectrographs of any resolution, high or low, including those too low to resolve laser frequency combs (LFC). We used a Michelson with multiple selectable interferometer delays, creating comb pitches proportional to the delay, to map out the Keck Planet Finder (KPF) spectrograph PSF width versus (X) wavelength and (Y) order #, during engineering tests at UC Berkeley Space Sciences Laboratory in early 2022. At that date the KPF laser frequency comb calibrator was not yet fully available due to shipping delays.

Keywords: high-resolution spectroscopy, spectrograph characterization

1. INTRODUCTION

1.1 Goals

The goal is to explore the ability of a small Michelson interferometer to diagnose the point spread function (PSF) of a high resolution spectrograph by measuring the sine fringe visibility across the detector chip. The novelty is that we measure the spectrograph response in frequency or Fourier space instead of the conventional method of measuring in pixel space using calibrants that have narrow linewidths.

1.2 Literature

The authors gained valuable insight into using the sine combs of white light Doppler interferometers since 1995,[1–5] and then extended expertise into astronomical spectroscopy.[6–10] (See for example discussion of sinusoidal comb filter behavior around Eq. 2 of Ref. 2.) The Keck Planet Finder spectrograph preliminary design is described by Ref. 11.

Author information:
D.J.E.: derskine@spectralfringe.org

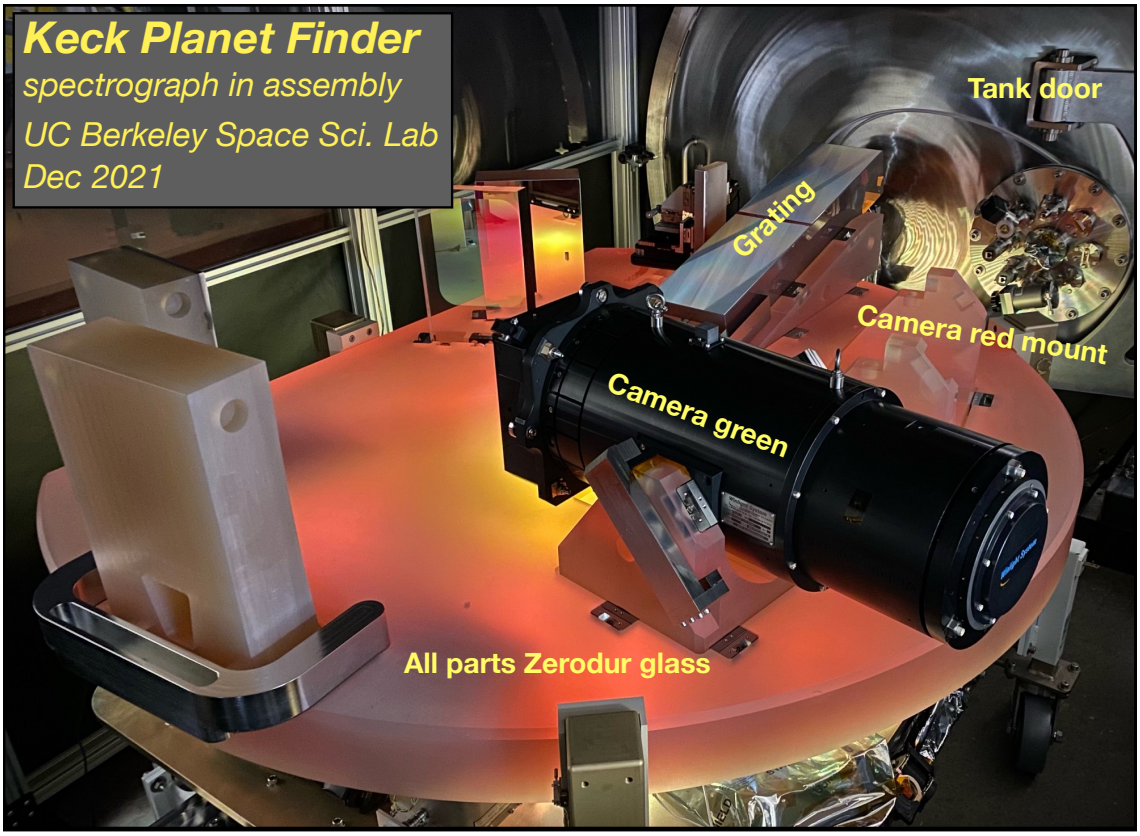

Figure 1. Keck Planet Finder spectrograph being assembled in high bay of Space Sciences Lab, UC Berkeley, December 2021. At time of photo the red camera has not yet been installed into its mount. Mounts and baseplate made of Zerodur glass to minimize thermal dilation.

1.3 Motivation during KPF assembly at UC Berkeley: needed PSF quickly

In January 2022, the Keck Planet Finder spectrograph (KPF) was undergoing initial assembly and engineering tests in the high bay at UC Berkeley Space Sciences Lab (Fig. 1). It needed to quickly check the quality of its focal point PSF (point spread function) in order to adjust alignment of internal optical components. But the KPF laser frequency comb (LFC) system that was to measure PSF width in the conventional manner was delayed shipping from Germany.

A Michelson interferometer (Fig. 2) was built in January 2022 for an independent spectroscopy project. We were alerted to the opportunity of applying it as an impromptu sine comb generator by illuminating it with white light, to help diagnose the performance of the Keck Planet Finder (KPF) spectrograph, coincidentaly being assembled in the building next door.

2. METHOD

Figure 3 shows schematic of experiment– a white light illuminated Michelson interferometer generates sine combs to diagnose Keck Planet Finder spectrograph. The Michelson can generate precise periodic combs, but of a sinusoidal shape rather than a series of narrow peaks like the laser frequency comb (LFC).

Sine combs injected into the KPF spectrograph probe its response to different well-defined spatial frequencies. Figure 4 shows that by measuring the relative magnitude of the detected sine comb fringe visibility versus frequency, we measure the modulation transfer function (MTF), which is the Fourier transform of the instrument PSF. Then in principle, the inverse Fourier transform of the MTF can reveal the KPF's Point Spread Function (PSF), or line spread function. In practice, it was simpler and expedient to fit two measured visibilities (the

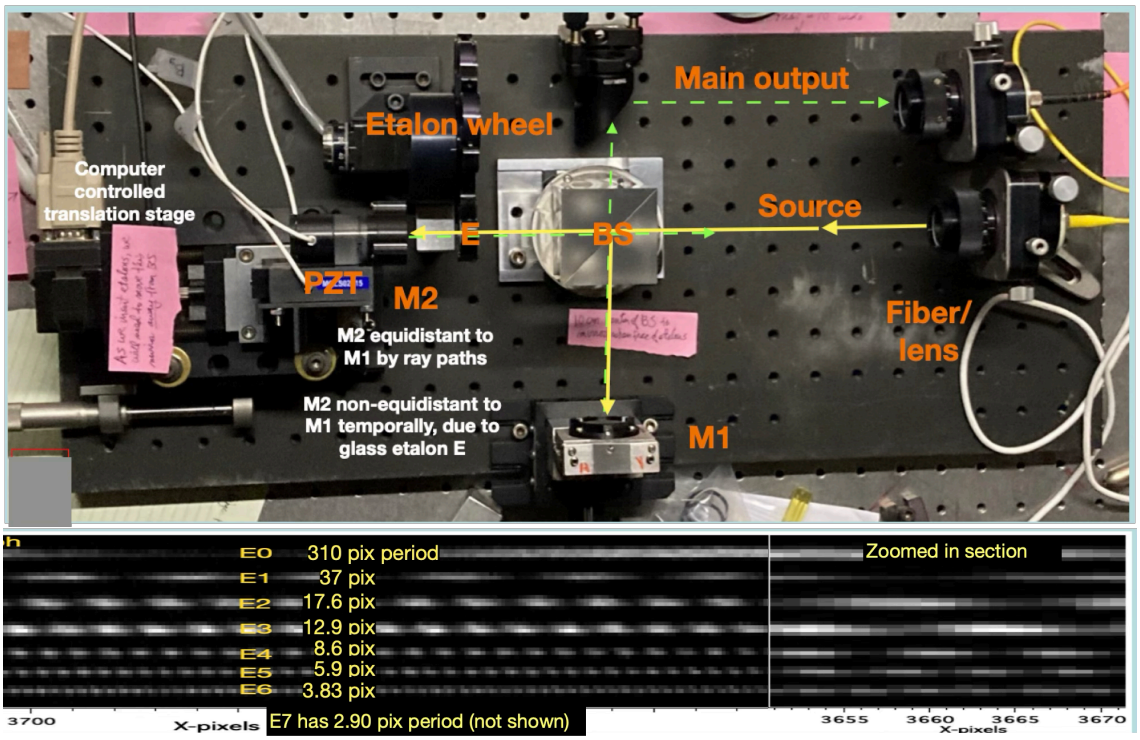

Figure 2. Selectable-delay Michelson interferometer makes sine combs on KPF at every pixel along the orders. The comb pitch (1/period) is proportional to the choice of glass etalon thickness (delay) inserted into one interferometer arm. Periodicities observed on the green camera, near the top of the detector chip at ∼600 nm, from delays E0-E7 in pixels were 310, 37, 17.6, 12.9, 8.6, 5.9, 3.83 and 2.90, with larger delays producing finer pitched (smaller period) sinusoids. (Comb of the largest delay E7 is not shown.) These periodicities will change with wavelength and camera. The two cameras are a "green" [445-600 nm], and a "red" [600-870 nm].

lowest delay E0 and some higher delay) to a Gaussian model to extract a full width at half max (FWHM) for the Gaussian peak in delay space, and then to pixel space.

The multi-delay capability of our Michelson, which was intended to measure high resolution spectra when starlight was injected into the Michelson, became useful as a way of generating sine combs of widely different spatial frequencies when white light illuminated the Michelson, to map out the MTF. Figure 5 shows the Michelson apparatus as used with the Keck Planet Finder. Being on a cafeteria cart, it is portable and fiber-optically connected to the KPF.

2.1 Our apparatus

The fixed delay wide angle[12] Michelson interferometer design used here with the 90 degree beamsplitter is similar to what we used[7] in the late 1990's, augmented by an additional 8-position filter wheel holding selectable glass etalons (as was done in the TripleSpec-Interferometer stellar observations at the Hale Telescope[9,10]). An interferometer cavity mirror was mounted on a PZT transducer to allow optional phase stepped data taking (to reduce fixed pattern noise at weakly illuminated chip edges), and was also on a computer controlled motorized stage so that the mirror position quickly moved to previously determined sweet spots for each etalon choice.

Other researchers have developed thermally stabilized monolithic interferometers (SMI) to make sine combs as a precision wavelength calibrant.[13–17] We did not use a SMI, since our main interest was not to calibrate the spectrograph to wavelength (others were doing that task), but to measure fringe visibility. Since the illumination was bright the exposure times were short (∼1 sec), so thermal drift during an exposure was not an issue.

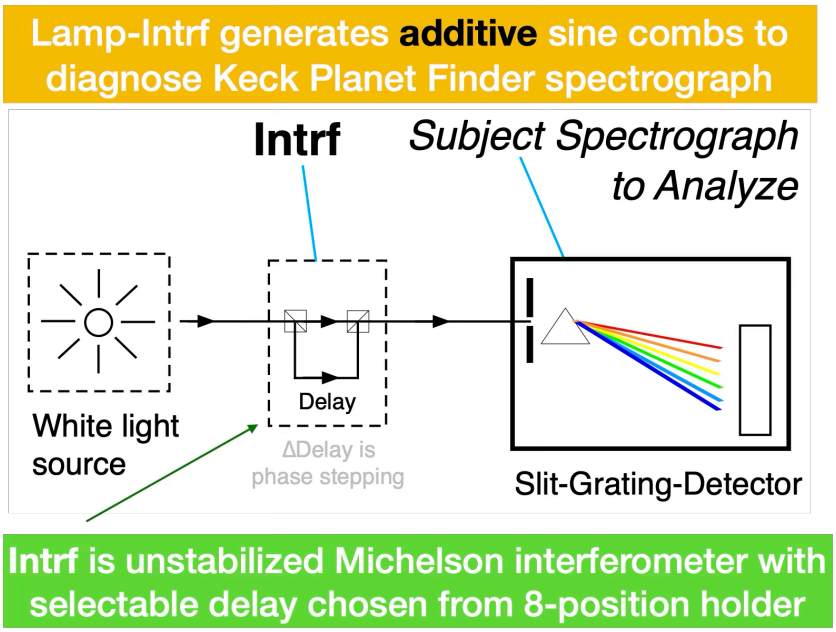

Figure 3. Schematic of experiment. White light lamp illuminated Michelson interferometer with a selectable delay τ (in units of cm) generates sine combs of relative intensity $I(\nu) = 0.5 * (1 + \sin 2\pi\tau\nu)$ to diagnose Keck Planet Finder spectrograph. The wavenumber (units cm^{-1}) $\nu = 1/\lambda$ is the preferred variable over wavelength, since it makes a periodic transmission comb in ν-space. The delay can be optionally incremented by a PZT transducer on a cavity mirror by a sub-wavelength amount $\Delta\tau$ in between several exposures to deliberately change the fringe phase (called "phase stepping"). This can help isolate a weak fringe signal from fixed pattern noise on edges of detector chip. For the majority of the chip region, we found that a single exposure was easily sufficient to measure the sine fringe visibility, especially when sine-fitted over a group of 200 pixels.

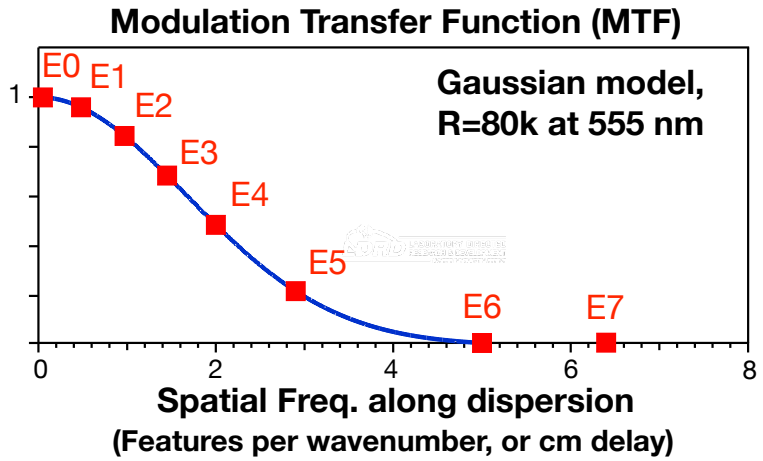

Figure 4. The theoretical modulation transfer function (MTF) measures spectrograph performance in Fourier space (features per cm^{-1} or cm). Here calculated sine magnitudes (Y-axis) yield the frequency response. Fourier transform of a measured MTF in principle yields the PSF shape in wavenumber space, which can be converted to pixel space. This graphic is calculated for resolving power of 80k at λ= 555 nm, hence for the green camera. Since the data shown later was taken on the red camera (600 to 870 nm) instead of green camera, the behavior will have different horizontal scale for the same resolving power. Delays E0 to E7 in cm, were 0.06, 0.51, 1.08, 1.47, 2.21, 3.30, 4.86, 6.41 for 555 nm (dispersion in glass will slightly alter delays for red camera).

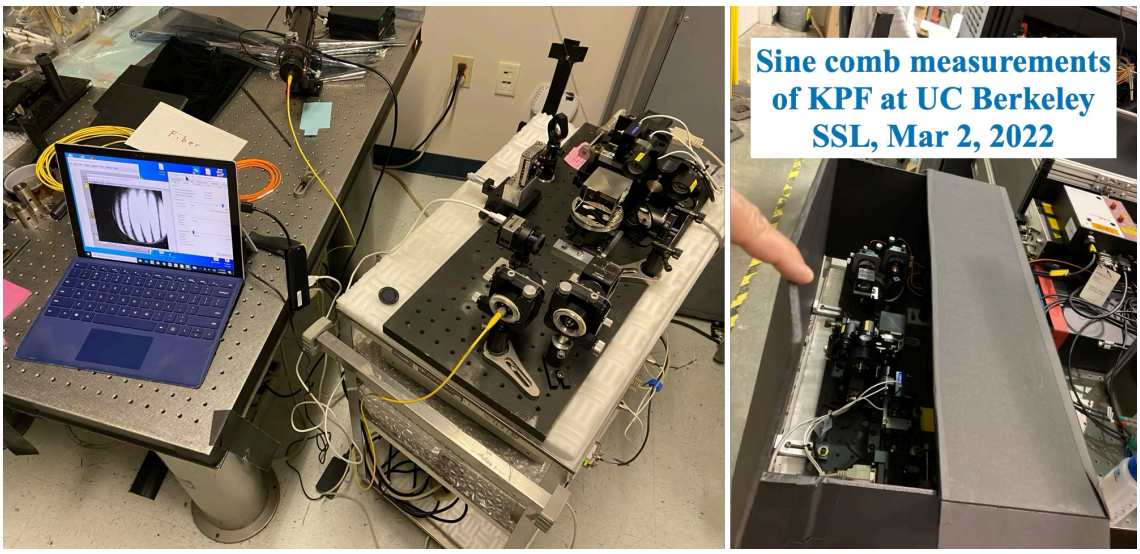

Figure 5. The Michelson interferometer was assembled in a few days in spring of 2022 from hand-me-down parts. It was portable and fiberoptically connected to the KPF. A cafeteria-cart, with foam underneath the metal optical breadboard to reduce vibrations, supported it while it generated sine combs for diagnosis of the Keck Planet Finder's PSF. This was sufficient due to the short exposure times (1 sec) used with the bright white light source.

2.1.1 Single exposure yields FWHM over a group of pixels

We elected to average the sinusoidal fringing visibility over groups of 200 pixel blocks for simplicity of display and analysis, since that allowed use of a single exposure.

2.1.2 Optional phase stepped exposures yield FWHM for a pixel

However we also took a full set of phase stepped exposures in case we decided to analyze the data in that manner, which offers better rejection of fixed pattern noise for the portion of the data that is weak at the edges of the detector chip. Phase stepping also allows analyzing fringe visibility at each individual pixel (by comparing maximum to minimum intensity change when interferometer phase changes 180 degrees.)

2.1.3 Delay values

Delays E0-E7 have values 0.06, 0.51, 1.08, 1.47, 2.21, 3.30, 4.86, and 6.41 cm. They have sine periodicities on the green camera at ∼600 nm of 310, 37, 17.6, 12.9, 8.6, 5.9, 3.83 pixels, for E0-E7.

2.2 Advantages of the Modulation Transfer Function (MTF) method

- White light lamp extends past blue limit (480 nm) of KPF Laser Frequency Comb.
- Measures every pixel along dispersion axis (no gaps such as in a spectral lamp).
- Can measure high or low resolution systems, since delay is selectable.
- Inexpensive: built from hand-me-down parts in a few days.
- Portable, robust, (Fig. 5) fiber-optically connected to spectrograph.
- Intrinsic linewidth W_0 of a spectral calibrant not needed, as in Eq. 1 for conventional method, which convolves FWHM of calibrant and instrument in dispersion space.

$$W^2_{instrm} = W^2_{msrd} - W^2_0. \quad (1)$$

. • It takes time exposure in the same manner as in regular stellar usage at an observatory (i.e. is not a Fourier Transform Spectrometer with a scanning delay requiring high temporal frequency detectors).

- It can be used simultaneously with other standard diagnostic methods of LFC or spectral lamps.

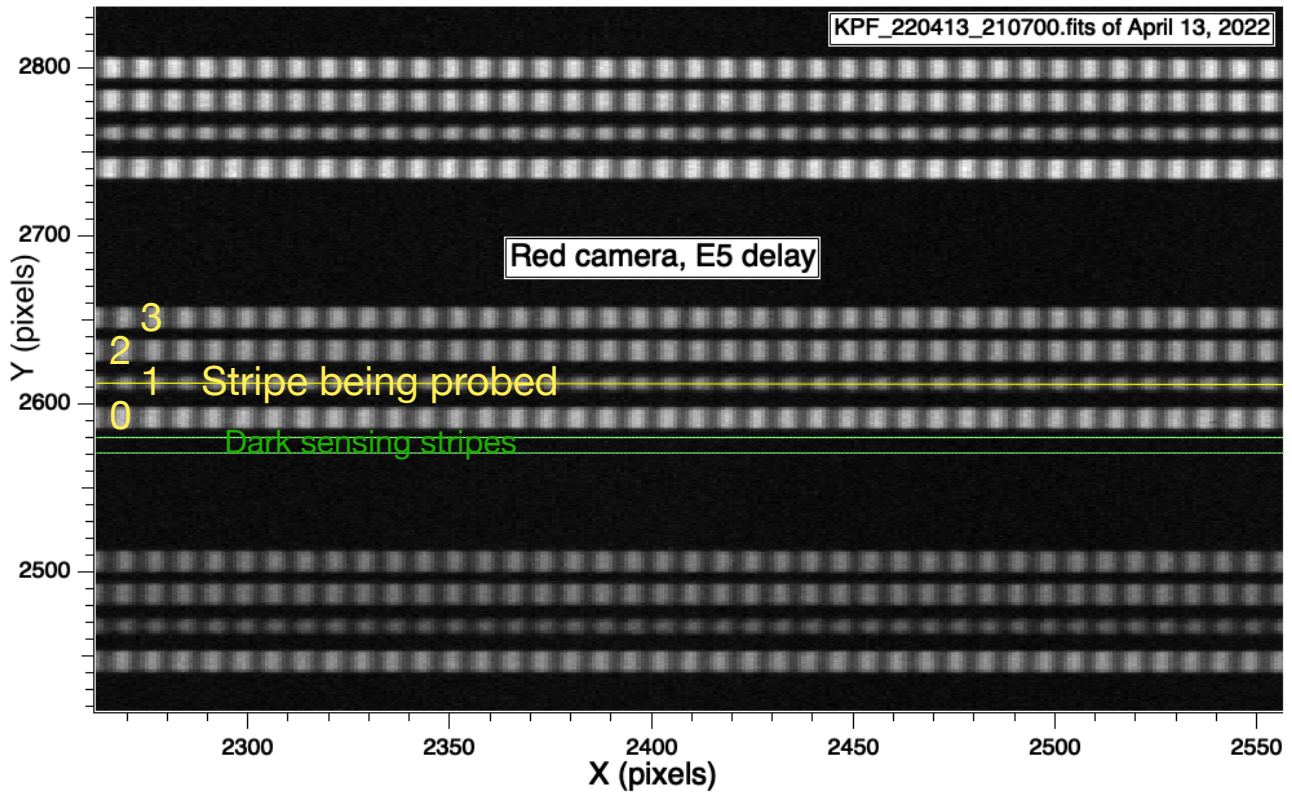

Figure 6. Example comb data, for interferometer delay E5 on the red camera detector chip, recorded April 13, 2022, with 1 sec exposure time. Since light passes through the same interferometer, combs are simultaneously created on all four of the optical fibers illuminating the spectrograph. For this proceedings we are analyzing the fiber which is 2nd from bottom ("Stripe1"), for an order approximately at Y∼2660 (order# = 22). To subtract the background, we also measure a couple lineouts shown as green lines "Dark sensing stripe") on an adjacent area immediately neighboring the four data stripes.

3. RESULTS

3.1 First light sine combs

First light for KPF sine combs was March 2, 2022, on the green camera (445 - 600 nm), when the red camera (600 - 870 nm) was not yet available. Sine combs were first recorded on the red camera April 13, 2022.

3.2 Example results for red camera

Figure 6 shows example of a comb, for interferometer delay E5, on the red camera detector chip. Figure 7 shows initial of analysis of a comb that separates it from background. Figure 8 shows a sine fit of a comb to determine its fringe visibility, over about 200 pixel region.

Figure 9 shows Gaussian fits for the red camera, for 3 combs (using delays E5, E6 and E7) as they span across chip in X-direction, for order Y∼2660 (λ ∼760 nm) and stripe # 1. Note that the comb spatial frequency changes across detector X=0 to X=4000 pix, mainly due to spectrograph behavior.

The E0 delay (quasi-zero fringe frequency) establishes the Gaussian model height. Each individual delay visibility (E5, E6, E7) yields a value for the MTF's FWHM when compared to E0 visibility, using the simple Gaussian model.

3.3 PSF FWHM maps vs X,Y position on detector

Figure 10 shows (X,Y) maps of the so-obtained FWHM for the red camera for delays E5, E6, and E7. The Y-axis is the order #, and the X-axis are in blocks of 200 pixels along dispersion. This shows how the PSF varies spatially across the many orders.

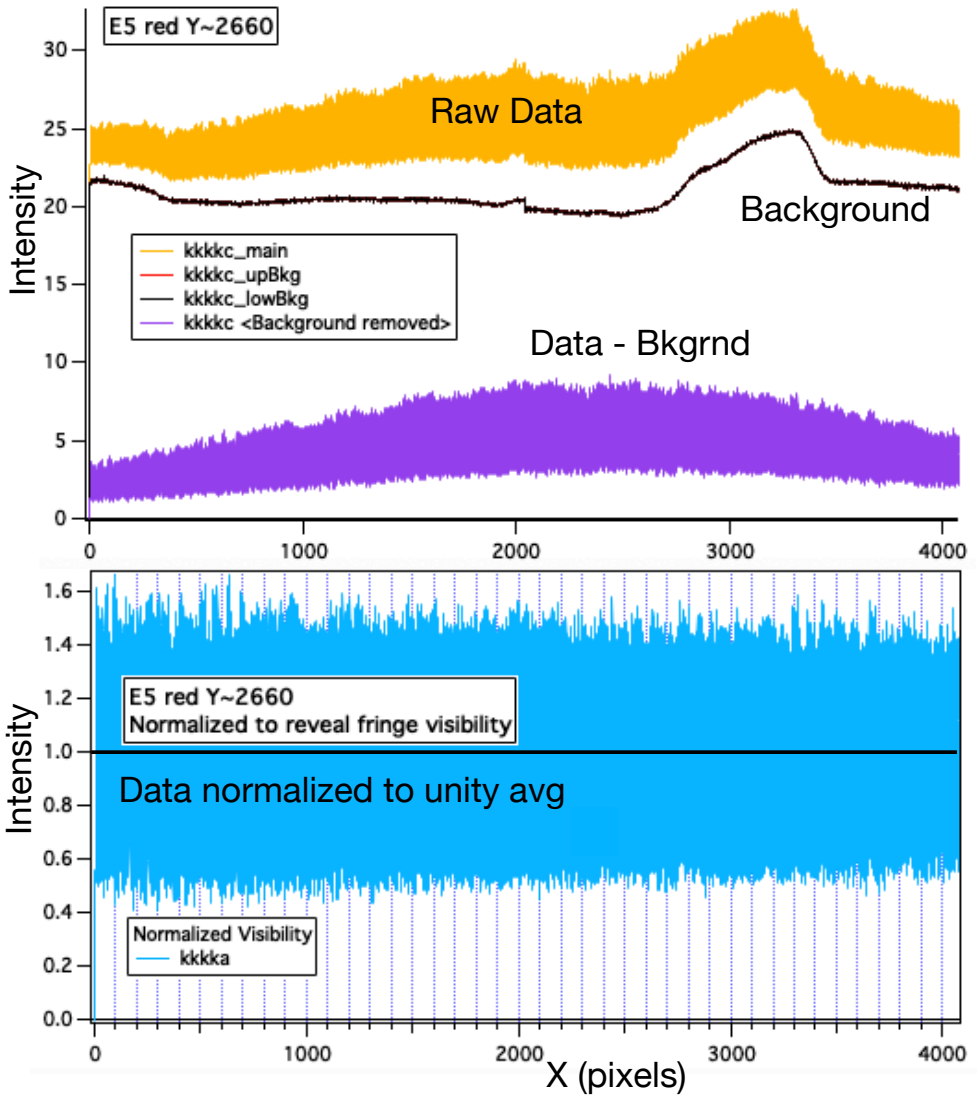

Figure 7. Example analysis of a comb along the order for E5 and order# 22 (same data as in Fig. 6). Gold is raw line out, black and red curves (nearly superimposed) show dark lineouts, and purple shows data after subtraction of averaged dark. Blue is after the slowly curving trend is subtracted from data, so that residual has an average value of unity.

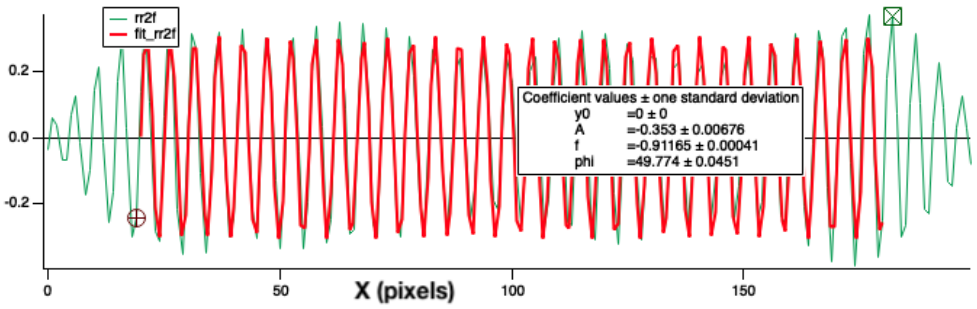

Figure 8. Example sine fit of a comb to determine its fringe visibility, over about 200 pixel region. Sine fitting could be done over a smaller region, but averaging over a 200 pixel region simplifies the maps being displayed below.

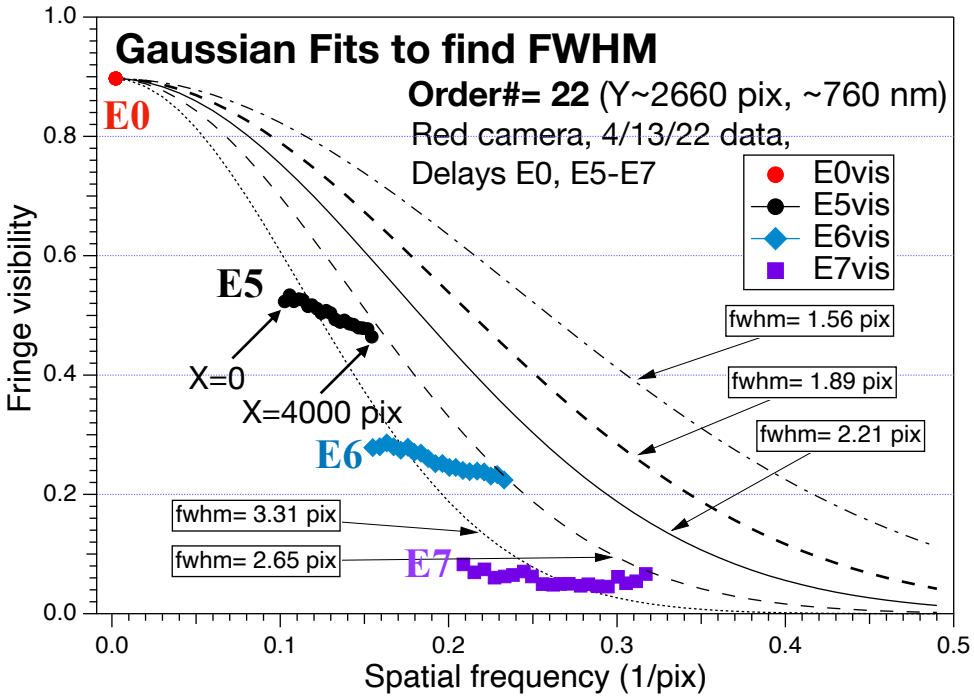

Figure 9. Gaussian fits for the red camera, for three delays E5, E6 and E7, stripe # 1, for order# 22, Y∼2660 (λ ∼760 nm). Note that the pitch (horizontal axis in waves per pixel) of the comb changes versus gross wavenumber due to spectrograph behavior. This creates the nonzero horizontal extent of the groups of data for each delay E5, E6, E7, in this visibility versus spatial frequency plot. Data taken April 13, 2022.

4. DISCUSSION

4.1 Conventional method: intrinsic linewidth W_0 of calibrant needed

For the conventional method, the spectrograph broadening (W_{instrm}) is learned by measuring a net linewidth (W_{msrd}). The latter is a convolution between the instrinsic linewidth (W_0) of the source (calibrant), and the instrument W_{instrm}, as $W_{msrd}^2 = W_{instrm}^2 + W_0^2$. Hence (assuming Gaussian PSF), the instrument behavior is

$$W_{instrm}^2 = W_{msrd}^2 - W_0^2. \tag{2}$$

If W_0 is not known and zero substituted for simplicity, then W_{instrm} tends to be overestimated and spectrograph resolution underestimated. This issue becomes significant for the highest resolutions when W_{instrm} becomes small, $W_0 \geq 0.3 W_{instrm}$. (The intrinsic linewidth may be hard to measure accurately, since it requires a technique or spectrograph of even higher resolution than the one being tested.) For low resolution spectrographs where $W_{instrm} \gg W_0$, then $W_{msrd} \approx W_{instrm}$ is a reasonable approximation.

4.2 MTF method: visibility of asymtopically small delay (E0) needed

For the sine comb method an intrinsic quantity is also needed, but it is the continuum fringe visibility which establishes the height of the Gaussian MTF shape at zero delay or pitch. This is easy to measure using a very small delay E0 of 0.06 cm, which generates a very broad periodicity of ∼310 pixels (at 600 nm). This pitch is much smaller than the width of the Gaussian MTF and so is a good measure of its height at zero pitch.

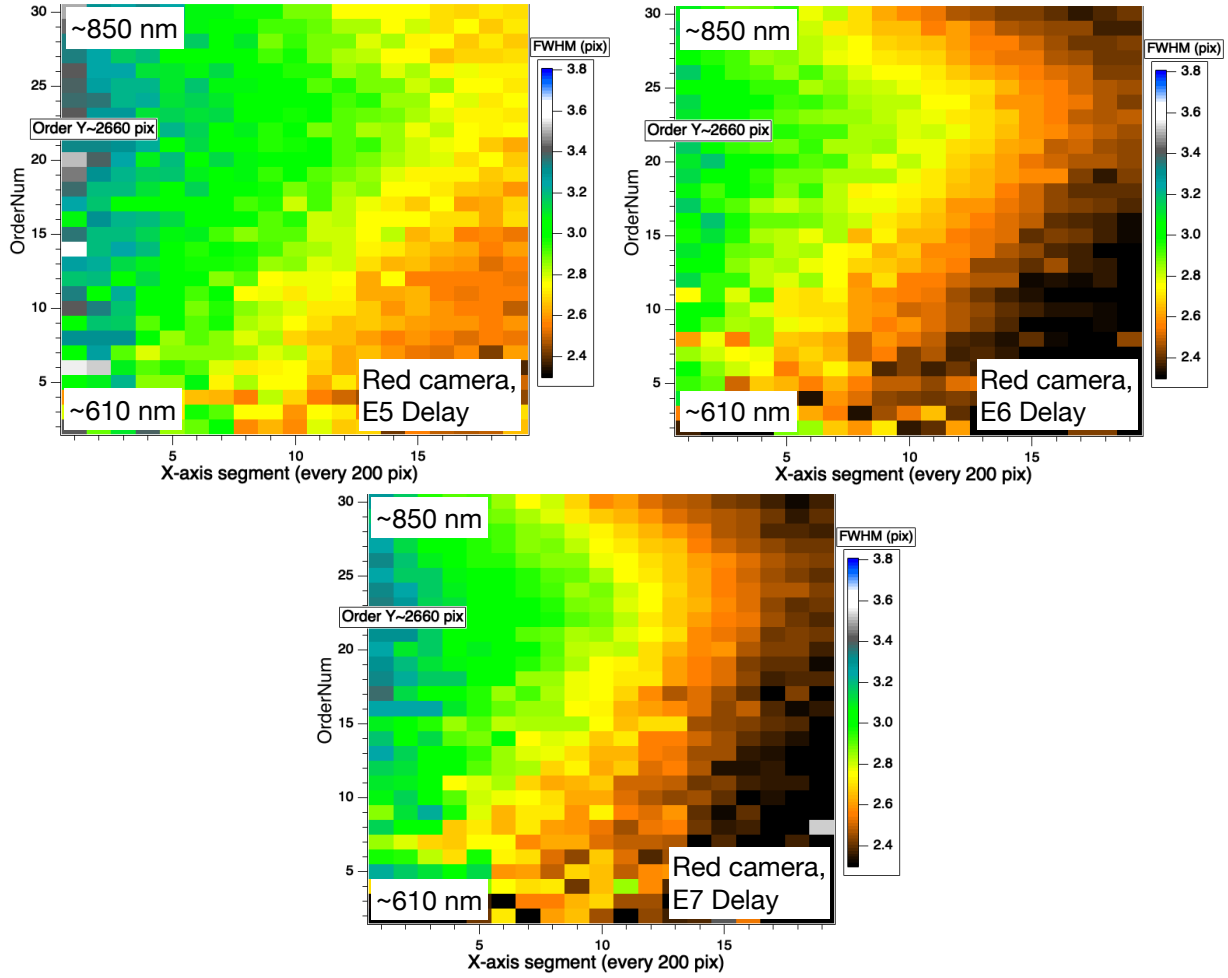

Figure 10. Results for red camera measured April 13, 2022 for three etalons E5, E6, E7, and stripe # 1 (2nd from bottom of the four fibers. These three etalons were independently measured but in rapid succession. The Y-axis ranges ∼610 to ∼850 nm, bottom to top. Each X-axis unit represents 200 pixels along order on detector. Color legend ("PlanetEarth" sequence of colors) on right hand side shows a Gaussian full width at half max (FWHM) in pixels ranging from 2.3 (black) to 3.8 (blue).

5. CONCLUDING REMARKS

5.1 Take-away thoughts

An inexpensive Michelson interferometer, fiber connected, created sine combs that illuminated every pixel of every spectrograph order. The components that make the Michelson inteferometer can be found in many university optics labs.

The sine comb magnitude shows at once how a spectrograph point spread function (PSF) varies across the detector chip, which is a useful diagnostic for adjusting the spectrograph optics for maximum performance. This method would work for spectrographs of any resolution, high or low, including those that cannot resolve laser frequency combs.

We measured the Keck Planet Finder spectrograph PSF width over its detector chip. Results for the three delays E5, E6, E7 were independently measured, yet consistent with each other.

Funding for this task was very brief. Furthering this preliminary work would make an interesting project useful to the spectroscopy community.

6. ACKNOWLEDGMENTS

Thanks to Sarah Blunt for processing of KPF wavelength calibration data. Some work prepared by LLNL under Contract DE-AC52-07NA27344, and supported by Laboratory Directed Research and Development project 22-LW-020. The Keck Planet Finder is supported by the Heising-Simons Foundation, the National Science Foundation, private donors, the Keck Foundation, the Simons Foundation, the Mt. Cuba Foundation, the Jet Propulsion Laboratory, the University of California Berkeley, the California Institute of Technology, the University of Hawaii, and the W.M. Keck Observatory.

REFERENCES

[1] D. J. Erskine and N. C. Holmes, "White Light Velocimetry," *Nature* **377**(6547), 317–320 (1995); https://doi.org/10.1038/377317a0

[2] D. J. Erskine and N. C. Holmes, "Imaging white-light VISAR," in *22nd International Congress on High-Speed Photography and Photonics*, D. L. Paisley, Ed., *Proc. SPIE* **2869**, 1080–1083 (1997); https://doi.org/10.1117/12.273416

[3] D. J. Erskine, "Techniques in broadband interferometry," Tech. Rep. UCRL-TR-201695, Lawrence Livermore Nat. Lab. (2004); https://doi.org/10.2172/15009760

[4] D. J. Erskine, "White Light Velocity Interferometer," *US Patent* **5,642,194** (1997).

[5] D. J. Erskine, "Single and Double Superimposing Interferometer Systems," *US Patent* **6,115,121** (2000).

[6] D. J. Erskine, "Combined dispersive/interference spectroscopy for producing a vector spectrum," *US Patent* **6,351,307** (2002).

[7] D. J. Erskine and J. Ge, "Novel Interferometer Spectrometer for Sensitive Stellar Radial Velocimetry," in *Imaging the Universe in Three Dimensions: Astrphys. Advncd. Multi-Wavel. Imaging Devices*, W. van Breugel and J. Bland-Hawthorn, Eds., *ASP Conf. Series* **195**, 501–507 (2000); http://digital.library.unt.edu/ark:/67531/metadc780974/

[8] D. J. Erskine, "An Externally Dispersed Interferometer Prototype for Sensitive Radial Velocimetry: Theory and Demonstration on Sunlight," *PASP* **115**, 255–269 (2003).

[9] P. S. Muirhead, J. Edelstein, D. J. Erskine, J. T. Wright, M. W. Muterspaugh, K. R. Covey, E. H. Wishnow, K. Hamren, P. Andelson, D. Kimber, T. Mercer, S. P. Halverson, A. Vanderburg, D. Mondo, A. Czeszumska, and J. P. Lloyd, "Precise Stellar Radial Velocities of an M Dwarf with a Michelson Interferometer and a Medium-Resolution Near-Infrared Spectrograph," *PASP* **123**, 709 (2011).

[10] D. J. Erskine, J. Edelstein, E. H. Wishnow, M. Sirk, P. S. Muirhead, M. W. Muterspaugh, J. P. Lloyd, Y. Ishikawa, E. A. McDonald, W. V. Shourt, and A. M. Vanderburg, "High-resolution broadband spectroscopy using externally dispersed interferometry at the Hale telescope: part 1, data analysis and results," *Journal of Astronomical Telescopes, Instruments, and Systems* **2**, 025004 (2016).

[11] S. R. Gibson, A. W. Howard, A. Roy, C. Smith, S. Halverson, J. Edelstein, M. Kassis, E. H. Wishnow, M. Raffanti, S. Allen, J. Chin, D. Coutts, D. Cowley, J. Curtis, W. Deich, T. Feger, D. Finstad, Y. Gurevich, Y. Ishikawa, E. James, E. Jhoti, K. Lanclos, S. Lilley, T. Miller, S. Milner, T. Payne, K. Rider, C. Rockosi, D. Sandford, C. Schwab, A. Seifahrt, M. M. Sirk, R. Smith, J. Stuermer, M. Weisfeiler, M. Wilcox, A. Vandenberg, and P. Wizinowich, "Keck Planet Finder: preliminary design," in *Ground-based and Airborne Instrumentation for Astronomy VII*, C. J. Evans, L. Simard, and H. Takami, Eds., **10702**, 107025X, International Society for Optics and Photonics, SPIE (2018).

[12] R. Hilliard and G. Shepherd, "Wide-Angle Michelson for Measuring Doppler Line Widths," *J. Opt. Soc. Am.* **56**, 362 (1966).

[13] S. Mahadevan, J. Ge, S. W. Fleming, X. Wan, C. DeWitt, J. C. van Eyken, and D. McDavitt, "An inexpensive field-widened monolithic michelson interferometer for precision radial velocity measurements," *PASP* **120**, 1001–1015 (2008).

[14] X. Wan and J. Ge, "Monolithic Michelson Interferometer as ultra stable wavelength reference," in *Optical and Infrared Interferometry II*, W. C. Danchi, F. Delplancke, and J. K. Rajagopal, Eds., **7734**, 77343N, International Society for Optics and Photonics, SPIE (2010).

[15] X. Wan, J. Ge, and Z. Chen, "Development of stable monolithic wide-field michelson interferometers," *Appl. Opt.* **50**, 4105–4114 (2011).

[16] J. Wang, J. Ge, X. Wan, N. De Lee, and B. Lee, "Accurate Group Delay Measurement for Radial Velocity Instruments Using the Dispersed Fixed Delay Interferometer Method. II. Application of Heterodyne Combs Using an External Interferometer Filter," *PASP* **124**, 1159 (2012).

[17] Xiaoke Wan and Jian Ge, "Stable monolithic interferometer for wavelength calibration," *US Patent* **8,570,524** (2013).